Lattice Boltzmann simulation of thermal nonideal fluids

G. Gonnella
Dipartimento di Fisica, Università di Bari and Istituto Nazionale di Fisica Nucleare, Sezione di Bari, via Amendola 173, 70126 Bari, Italy

A. Lamura
Istituto Applicazioni Calcolo, CNR, via Amendola 122/D, 70126 Bari, Italy

V. Sofonea
Center for Fundamental and Advanced Technical Research, Romanian Academy, Bd. Mihai Viteazul 24, 300223 Timişoara, Romania

(Received 19 February 2007; revised manuscript received 14 May 2007; published 7 September 2007)

A thermal lattice Boltzmann model for a van der Waals fluid is proposed. In the continuum, the model reproduces at second order of a Chapman-Enskog expansion, the theory recently introduced by A. Onuki [Phys. Rev. Lett. **94**, 054501 (2005)]. Phase separation has been studied in a system quenched by contact with external walls. Pressure waves favor the thermalization of the system at initial times and the temperature, soon with respect to typical times of phase separation, becomes homogeneous in the bulk. Alternate layers of liquid and vapor form on the walls and disappear at late times.

DOI: 10.1103/PhysRevE.76.036703 PACS number(s): 47.11.−j, 64.70.Fx, 05.70.Ln, 47.20.Hw

I. INTRODUCTION

In fluid systems the coupling between hydrodynamics and thermodynamics produces a variety of complex effects of fundamental and technological importance [1]. An example is the piston effect consisting of the speeding up of the thermal equilibration of a near-critical fluid warmed by external walls [2,3]. This is due to pressure waves created by thermal expansion near the walls. In phase transitions, heat transport and thermal gradients, often neglected, can be quite relevant [4,5]. When a fluid is quenched from a temperature above the critical point into a coexistence region, the temperature jump is generally assumed instantaneous in all of the system, and most of the theories are based on isothermal evolution [6]. However, in realistic situations, the system is quenched by contact with colder external walls. The temperature of the bulk does not set immediately at the value of the walls and this can influence the phase separation. Simulations are generally useful for analyzing these phenomena, but a full thermohydrodynamic study has been so far not considered.

An efficient approach to numerical simulations of fluids, which has been developed in the last years, is based on the so-called lattice Boltzmann method (LBM) [7]. A set of distribution functions representing densities of particles moving along fixed lattice directions evolve following Boltzmann equations with collision terms linearized in a single relaxation time approximation [8]. Conservation laws and proper choice of equilibrium distribution functions in the collision terms ensure that the correct hydrodynamic equations are recovered in the continuum limit. LBM has been applied to study single fluids, dynamics and phase ordering in multicomponent and complex fluids [9]; the method can easily handle complex geometries and is suitable for parallel implementation [7].

In this paper, inspired by the Klimontovich approach to kinetic theory for nonideal gases [10], we introduce a lattice Boltzmann scheme which allows to simulate the thermohydrodynamic equations for a multiphase fluid including interface free-energy contributions. This is an example of LBM able to correctly reproduce in the continuum, at second order of a Chapman-Enskog expansion, the transport equations recently established by Onuki [11]. We will study the phase separation of a van der Waals fluid. Our results show that thermalization occurs faster due to the "piston effect." After a very early stage of phase separation the temperature in the bulk of the system can be considered homogeneous. Alternate layers of liquid and vapor form close to the external walls, but do not survive at late times.

LBM for thermal fluids has been so far only set up for ideal fluids [12] or do not consider all terms present in continuum equations [13]. We define density, velocity, and temperature as momenta of various orders of the same set of particle distributions—see Eqs. (1)–(3). In other models, where the temperature results form a separate set of distributions, the energy equation reduces to a convection-diffusion equation not including all the stress contributions [14]. Moreover, the Prandtl number can be varied in our model, and due to the large variability of this number in real systems, this is a major goal in LBM for nonideal fluids [12]. We will use a finite difference lattice Boltzmann method (FDLBM) [15], where the relationship $c=\delta s/\delta t$ among the lattice speed c and the space and time steps δs and δt are no longer considered. In thermal LBM, for each direction, different distribution functions are introduced moving with different speeds and FDLBM allows to choose the more convenient discrete velocity sets [16]. In addition, FDLBM enables to use different discretization schemes. This is useful for improving numerical stability and when nonuniform grids or mixtures with different masses are considered.

II. THE MODEL

We generalize the two-dimensional lattice Boltzmann model introduced in Ref. [16]. There are four sets of velocities defined by $\{\mathbf{e}_0=0, \mathbf{e}_{ki}=[\cos(i-1)\frac{\pi}{4}, \sin(i-1)\frac{\pi}{4}]c_k\}$ with

 ©2007 The American Physical Society

$k=1,\ldots,4; i=1,\ldots,8$. The values of the speeds c_k may be determined by asking for the largest temperature interval centered around $T_c=1$ (the critical temperature in our model) where the equilibrium distribution functions f_{ki}^{eq} are positive when the fluid velocity u is negligible [16]. We found the values $\{c_1,c_2,c_3,c_4\}=\{1.00,1.90,2.90,4.30\}$ within the temperature range [0.5,1.5].

The local density n, velocity $\mathbf{u}$, and temperature T are determined from the distribution functions f_{ki}, defined in each node of the lattice, as

$$n=\sum_{ki} f_{ki}, \tag{1}$$

$$nu_\alpha=\sum_{ki} f_{ki}e_{ki\alpha}, \tag{2}$$

$$n\left(T+\frac{u^2}{2}\right)=\frac{1}{2}\sum_{ki} f_{ki}c_k^2. \tag{3}$$

The functions f_{ki} evolve according to the equations

$$\partial_t f_{ki}+e_{ki\alpha}\partial_\alpha f_{ki}=-\frac{1}{\tau}[f_{ki}-f_{ki}^{\mathrm{eq}}]+I_{ki}, \tag{4}$$

where the first term on the right-hand side is the collision operator with relaxation time τ [8]. The $\{f_{ki}^{\mathrm{eq}}\}$'s are derived from the Maxwell distribution retaining up to fourth-order terms of flow velocity [16]. They are required to fulfill Eqs. (1)–(3) in order to guarantee mass, momentum, and energy conservation. We solve numerically Eq. (4) on a lattice of size $L\times W$ by using the forward time stepping rule for $\partial_t f_{ki}$ and a second-order finite difference scheme for the convective term $e_{ki\alpha}\partial_\alpha f_{ki}$ based on flux limiters [17] which reduce unphysical numerical oscillations of the density. We adopted the monitorized central difference scheme which proved to be effective in reducing spurious numerical terms in the case of isothermal nonideal fluids [18]. The systems investigated are limited by rigid walls at the left-hand and right-hand sides, kept at fixed temperature. Diffuse reflection boundary conditions [19] are implemented in a version capable to impose the wall temperature allowing free evolution of the fluid density [20].

The extra term I_{ki} accounts for interparticle forces and is the main contribution of our model. It has a structure similar to the one introduced by Klimontovich [10] in kinetic theories for nonideal gases, that is

$$I_{ki}=-[A+B_\alpha(e_{ki\alpha}-u_\alpha)+(C+C_q)(e_{ki\alpha}-u_\alpha)^2]f_{ki}^{\mathrm{eq}}. \tag{5}$$

The introduction of I_{ki} allows to recover mass, momentum, and energy equations of a van der Waals fluid [11],

$$\partial_t n=-\partial_\alpha(nu_\alpha), \tag{6}$$

$$\partial_t(nu_\alpha)=-\partial_\beta(nu_\alpha u_\beta)-\partial_\beta(\Pi_{\alpha\beta}-\sigma_{\alpha\beta}), \tag{7}$$

$$\partial_t e_T=-\partial_\alpha[e_T u_\alpha+(\Pi_{\alpha\beta}-\sigma_{\alpha\beta})u_\beta]+\partial_\alpha(\kappa_T\partial_\alpha T), \tag{8}$$

where $\Pi_{\alpha\beta}=p^w\delta_{\alpha\beta}+\Lambda_{\alpha\beta}$ is the nonviscous stress; $p^w=\frac{3nT}{3-n}-\frac{9}{8}n^2$ is the van der Waals pressure with a critical point at $T_c=n_c=1$, and $\Lambda_{\alpha\beta}=M\partial_\alpha n\partial_\beta n-M\left(n\nabla^2 n+\frac{|\nabla n|^2}{2}\right)\delta_{\alpha\beta}-\left[nT\partial_\gamma n\partial_\gamma\left(\frac{M}{T}\right)\right]\delta_{\alpha\beta}$ is the contribution to the pressure tensor depending on density gradients. $\sigma_{\alpha\beta}=\eta(\partial_\alpha u_\beta+\partial_\beta u_\alpha-\partial_\gamma u_\gamma\delta_{\alpha\beta})+\zeta\partial_\gamma u_\gamma\delta_{\alpha\beta}$ is the dissipative stress tensor with shear and bulk viscosities η and ζ [21]. The total energy density is $e_T=nT-\frac{9}{8}n^2+K\frac{|\nabla n|^2}{2}+nu^2/2$, and the expression $M=K+HT$ (K and H constants) allows a dependence of the surface tension on temperature.

We determine the contributions due to the term I_{ki} to the mass, momentum, and energy equations which read as

$$\sum_{ki} I_{ki}=A+2(C+C_q)T, \tag{9}$$

$$\sum_{ki} I_{ki}e_{ki\alpha}=-\{nu_\alpha[A+2(C+C_q)T]+nTB_\alpha\}, \tag{10}$$

$$\frac{1}{2}\sum_{ki} I_{ki}c_k^2=-\left\{n\left(T+\frac{u^2}{2}\right)[A+2(C+C_q)T]+2nT^2(C+C_q)+nTB_\alpha u_\alpha\right\}, \tag{11}$$

respectively. Starting from Eq. (4), we perform the Chapman-Enskog expansion with respect to the Knudsen number $\mathrm{Kn}=c_1\tau/L\delta s$ [7] to obtain the continuum equations. We fix the coefficients in (5) in order to recover Eqs. (6)–(8) by using Eqs. (9)–(11) which give the nonideal contributions.

By using the conservation laws and the structure of lattice vectors $\{\mathbf{e}_{ki}\}$, we find

$$A=-2(C+C_q)T, \tag{12}$$

$$B_\alpha=\frac{1}{nT}[\partial_\alpha(p^w-nT)+\partial_\beta\Lambda_{\alpha\beta}-\partial_\alpha(\zeta\partial_\gamma u_\gamma)], \tag{13}$$

$$C=\frac{1}{2nT^2}\left[(p^w-nT)\partial_\gamma u_\gamma+\Lambda_{\alpha\beta}\partial_\alpha u_\beta-(\zeta\partial_\gamma u_\gamma)\partial_\alpha u_\alpha+\frac{9}{8}n^2\partial_\gamma u_\gamma+K\left(-\frac{1}{2}(\partial_\gamma n)(\partial_\gamma n)(\partial_\alpha u_\alpha)-n(\partial_\gamma n)(\partial_\gamma\partial_\alpha u_\alpha)-(\partial_\gamma n)(\partial_\gamma u_\alpha)(\partial_\alpha n)\right)\right], \tag{14}$$

$$C_q=\frac{1}{2nT^2}\partial_\alpha[2qnT(\partial_\alpha T)]. \tag{15}$$

Equations (6)–(8) are obtained at the second order in Kn without extra spurious terms. The term C_q allows to tune the heat conductivity κ_T independently from the dynamic viscosity η. Indeed, we obtain $\eta=nT\tau$, $\kappa_T=2nT(\tau-q)$, so that the Prandtl number $\mathrm{Pr}=\eta/\kappa_T=\frac{\tau}{2(\tau-q)}$ can be varied by changing the parameter q keeping τ fixed. All of the terms (12)–(15) are readily computed in the code since they depend on the quantities n, $\mathbf{u}$, and T which are available at each time step. Derivatives are computed by using second-order finite difference schemes. The CPU time needed for our model is ap-

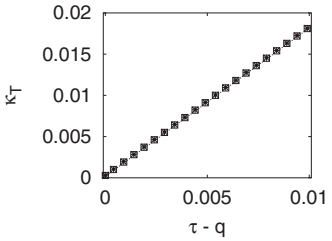

FIG. 1. Plot of the heat conductivity κ_T as a function of $\tau-q$ for $\delta s=0.01(*),0.002(\square)$. The parameter τ is fixed at value 10^{-4} and q is varied in the range $[-0.009\,90;0.000\,09]$. The dashed line corresponds to the analytical expression $\kappa_T=2nT(\tau-q)$.

proximatively 33% larger than that for the ideal gas model where the term I_{ki} is switched off.

III. NUMERICAL RESULTS

In order to validate our algorithm we first checked numerically the previous expression for κ_T. We considered the fluid in the single phase region and initialized the system with a temperature wave around $T=0.90$ at $n=0.1$ and walls at temperature $T_W=0.90$. Since Eq. (8) reduces to a simple diffusion equation if $u=0$, at each iteration of these simulations the fluid velocity was set to zero after the measure of T and the value of κ_T was deduced from the decay of the wave. We kept τ fixed at 0.0001 and q was varied in order to change Pr in the range [0.005;5]. Numerical results shown in Fig. 1 agree very well with theoretical predictions $\kappa_T=2nT(\tau-q)$. We did not find any significant dependence on the space step δs since results are almost identical for different choices of δs.

We then investigated how the equilibrium between liquid and vapor is reproduced in our model. Densities of the coexisting phases were numerically computed at different temperatures and compared to the theoretical values estimated by Maxwell construction. For $T\geqslant 0.85$, results are very close to the theoretical curve. Below this value, deviations appear which become larger when reducing T. An equilibrium density profile separating the two phases is shown in Fig. 2.

We used $L=150$, $W=10$, $\delta s=0.01$, $\delta t=10^{-5}$, $\tau=10^{-4}$, $K=10^{-6}$, $H=0$, and walls kept at temperature $T_W=0.90$. A well-known problem in LBM is the presence of spurious velocities at interfaces [18]. In the present thermal model, these velocities act as local sources of heat which must be dissipated through the system. As a consequence, the bulk temperature is slightly larger than the one fixed on the walls by less than 5%.

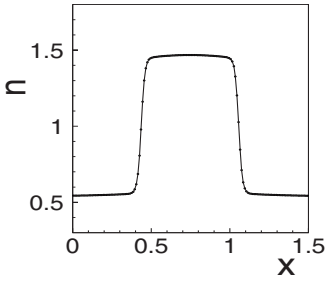

FIG. 2. Plot of density profile normal to two flat interfaces for a van der Waals fluid.

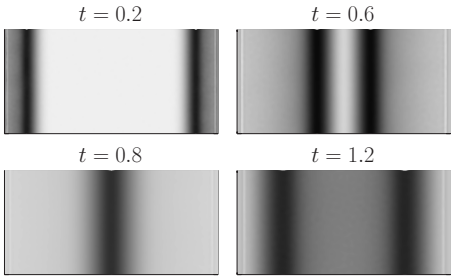

FIG. 3. Contour plots of pressure p^w at initial times of phase separation. Cold walls are placed on the left-hand and right-hand sides. Gray scaling from white→black corresponds to maximum p^w→minimum p^w.

We applied our LBM to study the phase separation of a van der Waals fluid, initially at $T>T_c$ with density n at each lattice node randomly chosen in the interval $[1.042-0.104;1.042+0.104]$, put in contact with colder walls at $T_W=0.90$. The value $n=1.042$ would give symmetric phase separation for an isothermal process with fully periodic boundaries. We used $L=512$, $W=256$, $\delta s=1/256$, $\delta t=10^{-5}$, $\tau=10^{-3}$, $q=-0.004$, $K=10^{-6}$, $H=0$. Thermal contraction close to the walls generates pressure waves which propagate as shown in Fig. 3. The waves move from the walls (see the figures at $t=0.2$ and $t=0.6$) towards the center of the system. After they come in contact, the waves separate generating a lower pressure between them ($t=1.2$). The two waves are later reflected from the walls; the process repeats and can be clearly observed in our simulations for three times until $t\sim 3$. This mechanism, also known as the piston effect, makes the thermalization of the system much faster than if only due to diffusion in the sense that in the bulk of the system, the temperature becomes very soon homogeneous with only a jump close to the walls. Our simulations show for the first time how it acts during phase separation [22], confirming the picture discussed in Ref. [1].

When the waves become negligible, temperature profiles like that of Fig. 4 are observed. Then, domains of the two

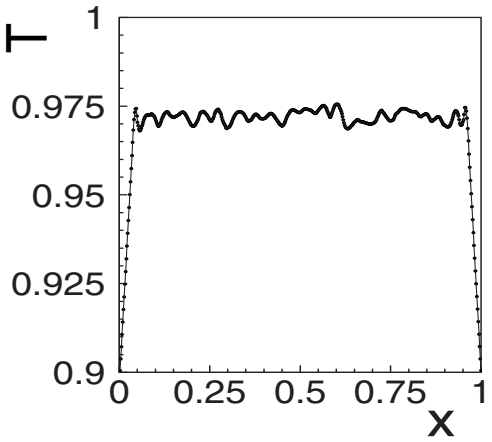

FIG. 4. Plot of the temperature profile across the system along a middle line at time $t=4$.

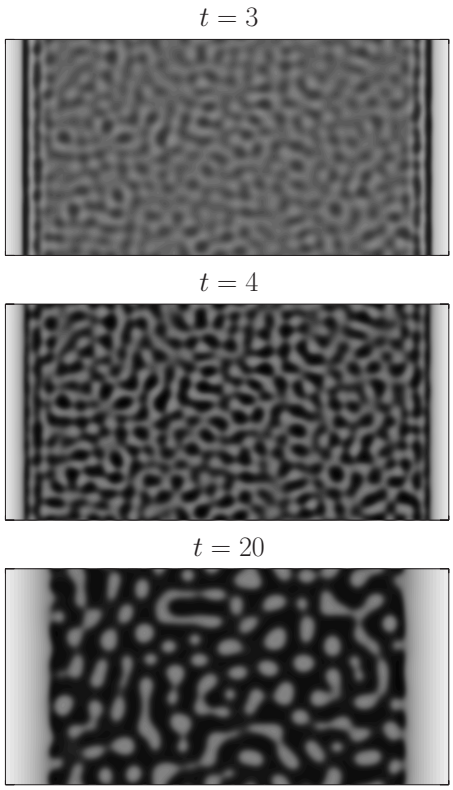

FIG. 5. Contour plots of density n at consecutive times during phase separation. Cold walls are placed on the left-hand and right-hand sides. Gray scaling from white→black corresponds to maximum n→minimum n.

phases start to form as shown in Fig. 5 at $t=3$. In the bulk the usual symmetric spinodal decomposition pattern can be observed, while layers of the denser phase condense on the walls. Actually, the liquid layer is followed by alternate layers of the two phases which, in all the cases examined with different τ and q, disappear at later times (see Fig. 5 at $t=4$). In previous simulations the alternate layers were observed to survive with time, but in those studies the temperature followed a prescribed time dependence [5] or was not properly coupled through hydrodynamic equations to the other state variables [23]. Moreover, we measured the growth of the width of the liquid layers on the walls and found a power law compatible with $t^{1/2}$.

Due to deposition of liquid on the walls (see Fig. 5 at $t=20$), the late time density patterns exhibit in the bulk the typical features of asymmetric quenching with the vapor playing the role of the majority phase. Liquid droplets become spherical and larger and larger; we did not find any dependence of growth rates on the viscosity and thermal conductivity. In the meantime, the temperature in the bulk decreases towards the wall values, slowly if compared with the growth of the droplet size. We could not appreciate changes in growth rate due to temperature variations in this last regime. Such patterns have been also observed in experiments for near-critical fluids [3,11].

IV. CONCLUSIONS

In conclusion, we have shown that LBM can be used to study the dynamics of van der Waals fluids dealing consistently with the thermodynamics of the systems. We studied the phase separation of a system put in contact with colder external walls showing the influence of thermal exchanges on the domain pattern evolution. Pressure waves at initial times favor the thermalization. We hope that our algorithm can be used to study other thermal effects in multiphase fluids. Improvements in the algorithm with further reduction of spurious velocities would allow to study systems subject to larger thermal gradients.

ACKNOWLEDGMENTS

The authors thank J. M. Yeomans for helpful discussions. The authors acknowledge support by INFLUS (Contract No. NMP3-CT-2006-031980), GAR 334 (2005–2006), and INFM for using CINECA Consortium for Supercomputing.

[1] A. Onuki, *Phase Transition Dynamics* (Cambridge University Press, Cambridge, 2002).
[2] A. Onuki, H. Hao, and R. A. Ferrell, Phys. Rev. A **41**, 2256 (1990).
[3] H. Boukari, M. E. Briggs, J. N. Shaumeyer, and R. W. Gammon, Phys. Rev. Lett. **65**, 2654 (1990); Y. Garrabos, M. Bonetti, D. Beysens, F. Perrot, T. Frohlich, P. Carles, and B. Zappoli, Phys. Rev. E **57**, 5665 (1998), and references therein.
[4] J. P. Donley and J. S. Langer, Phys. Rev. Lett. **71**, 1573 (1993).
[5] H.-O. Carmesin, D. W. Hermann, and K. Binder, Z. Phys. B: Condens. Matter **65**, 89 (1986).
[6] See, e.g., A. J. Bray, Adv. Phys. **43**, 357 (1994).
[7] S. Succi, *The Lattice Boltzmann Equation for Fluid Dynamics and Beyond* (Oxford University Press, Oxford, 2001).
[8] P. Bhatnagar, E. Gross, and M. Krook, Phys. Rev. **94**, 511 (1954).
[9] J. M. Yeomans, Annu. Rev. Comput. Phys. **7**, 61 (2000).
[10] Y. L. Klimontovich, *Kinetic Theory of Nonideal Gases and Nonideal Plasmas* (Pergamon, Oxford, 1982).
[11] A. Onuki, Phys. Rev. Lett. **94**, 054501 (2005); Phys. Rev. E **75**, 036304 (2007).
[12] F. J. Alexander, S. Chen, and J. D. Sterling, Phys. Rev. E **47**, R2249 (1993); C. Teixeira, H. Chen, and D. M. Freed, Comput. Phys. Commun. **129**, 207 (2000).
[13] R. Zhang and H. Chen, Phys. Rev. E **67**, 066711 (2003); T. Seta, K. Kono, and S. Chen, Int. J. Mod. Phys. B **17**, 169 (2003).
[14] B. J. Palmer and D. R. Rector, Phys. Rev. E **61**, 5295 (2000); T. Ihle and D. M. Kroll, Comput. Phys. Commun. **129**, 1 (2000).
[15] N. Cao, S. Chen, S. Jin, and D. Martinez, Phys. Rev. E **55**,

R21 (1997).
[16] M. Watari and M. Tsutahara, Phys. Rev. E **67**, 036306 (2003).
[17] E. F. Toro, *Riemann Solvers and Numerical Methods for Fluid Dynamics* (Springer-Verlag, Berlin, 1999).
[18] V. Sofonea, A. Lamura, G. Gonnella, and A. Cristea, Phys. Rev. E **70**, 046702 (2004).
[19] V. Sofonea and R. F. Sekerka, Phys. Rev. E **71**, 066709 (2005).
[20] V. Sofonea, Phys. Rev. E **74**, 056705 (2006); Europhys. Lett. **76**, 829 (2006).
[21] L. D. Landau and E. M. Lifshitz, *Fluid Mechanics* (Butterworth-Heinenann, Oxford, 1987).
[22] The droplet-interconnected domains transition has been studied in phase separation experiments in absence of gravity by F. Perrot, D. Beysens, Y. Garrabos, T. Frohlich, P. Guenoun, M. Bonetti, and P. Bravais, Phys. Rev. E **59**, 3079 (1999).
[23] R. C. Ball and R. L. H. Essery, J. Phys.: Condens. Matter **2**, 10303 (1990); H. W. Alt and I. Pawlow, Physica D **59**, 389 (1992).